PHYSICAL REVIEW A **91**, 062106 (2015)

Generalized Klein-Nishina formula

K. Krajewska,[1,2,*] F. Cajiao Vélez,[1] and J. Z. Kamiński[1]
[1]*Institute of Theoretical Physics, Faculty of Physics, University of Warsaw, Pasteura 5, 02-093 Warszawa, Poland*
[2]*Department of Physics and Astronomy, University of Nebraska, Lincoln, Nebraska 68588-0299, USA*
(Received 23 March 2015; published 8 June 2015)

The generalized Klein-Nishina formula for Compton scattering of charged particles by a finite train of pulses is derived in the framework of quantum electrodynamics. The formula also applies to classical Thomson scattering provided that frequencies of generated radiation are smaller that the cutoff frequency. The validity of the formula for incident pulses of different durations is illustrated by numerical examples. The positions of the well-resolved Compton peaks, with the clear labeling by integer orders, opens up the possibility of the precise diagnostics of properties of relativistically intense, short laser pulses. This includes their peak intensity, the carrier-envelope phase, and their polarization properties.

DOI: 10.1103/PhysRevA.91.062106 PACS number(s): 12.20.Ds, 12.90.+b, 42.55.Vc, 13.40.−f

I. INTRODUCTION

In order to understand the physics behind the interaction of strong laser pulses with matter, it is necessary to have well-characterized interacting pulses. With current technology, this is accomplished for laser fields in the optical regime provided that their intensity is no larger than 10^{15} W/cm^2. As pointed out by many authors (see, for instance, Refs. [1–7]), the same task becomes particularly challenging at higher intensities, where any direct measurement is prone to damaging the equipment. Therefore, different proposals were put forward to determine properties of ultrastrong and short laser pulses (e.g., the laser peak intensity [1–5,7] or the carrier-envelope phase [6]). As we argue in this paper, sensitivity of Compton scattering to the driving train of pulses can be traced back to the properties of pulses comprising the train. This can be based on the *generalized Klein-Nishina (GKN) formula*, which we derive in this paper.

A. Klein-Nishina formula

The original Klein-Nishina formula [8] for the Compton scattering with the electron initial four-momentum $p_{\rm i}$ [$p_{\rm i}\cdot p_{\rm i}=(m_{\rm e}c)^2$, where the centered dot denotes the relativistic scalar product, $a\cdot b=a^0b^0-a^1b^1-a^2b^2-a^3b^3=a^0b^0-\boldsymbol{a}\cdot\boldsymbol{b}$], has the form

$$\omega_{\boldsymbol{K}}=\frac{\omega}{\frac{p_{\rm i}\cdot n_{\boldsymbol{K}}}{p_{\rm i}\cdot n}+\frac{\omega}{\omega_{\rm cut}}}, \tag{1}$$

where $k=(\omega/c)n$ and $K=(\omega_{\boldsymbol{K}}/c)n_{\boldsymbol{K}}$ are the four-momenta of the initial and final photons, respectively, $n=(1,\boldsymbol{n})$, $n_{\boldsymbol{K}}=(1,\boldsymbol{n}_{\boldsymbol{K}})$, and $k\cdot k=K\cdot K=0$. In this equation,

$$\omega_{\rm cut}=\frac{cp_{\rm i}\cdot n}{\hbar n\cdot n_{\boldsymbol{K}}} \tag{2}$$

is the maximum frequency of photons generated in the Compton process.

Consider the Compton process which takes place in an intense monochromatic plane wave of the frequency ω, propagating in the direction $\boldsymbol{n}$. The vector potential of, in general, the elliptically polarized plane wave equals

$$A(k\cdot x)=A_0[\varepsilon_1\cos(k\cdot x)\cos\delta+\varepsilon_2\sin(k\cdot x)\sin\delta], \tag{3}$$

where ε_j ($j=1,2$) are two real polarization four-vectors normalized such that $\varepsilon_j\cdot\varepsilon_{j'}=-\delta_{jj'}$ and $k\cdot\varepsilon_j=0$. Without the loss of generality, we assume that the time components of these vectors are zero, i.e., $\varepsilon_j=(0,\boldsymbol{\varepsilon}_j)$. If the electron absorbs $N=1,2,\ldots$ photons from the plane wave it may emit, in the direction $\boldsymbol{n}_{\boldsymbol{K}}$, the Compton photon of frequency $\omega_{\boldsymbol{K},N}$ [9–14],

$$\omega_{\boldsymbol{K},N}=\frac{N\omega}{\frac{p_{\rm i}\cdot n_{\boldsymbol{K}}}{p_{\rm i}\cdot n}+\frac{U}{c}\frac{n\cdot n_{\boldsymbol{K}}}{p_{\rm i}\cdot n}+\frac{N\omega}{\omega_{\rm cut}}}, \tag{4}$$

where

$$U=\frac{1}{4}\mu^2\frac{(m_{\rm e}c^2)^2}{cp_{\rm i}\cdot n} \tag{5}$$

has the meaning of the ponderomotive energy of electrons in the laser field. Here, the relativistically invariant parameter,

$$\mu=\frac{|e|A_0}{m_{\rm e}c}, \tag{6}$$

determines the intensity of the electromagnetic plane wave. Both U and μ are the classical quantities, whereas the term proportional to $\omega/\omega_{\rm cut}$ in Eq. (4) accounts for the quantum recoil of electrons during the Compton process. Such a recoil of electrons does not take place in the corresponding classical process, called the Thomson scattering. This allows us to introduce into the Klein-Nishina formula the classical Thomson frequency,

$$\omega^{\rm Th}_{\boldsymbol{K},N}=\frac{N\omega}{\frac{p_{\rm i}\cdot n_{\boldsymbol{K}}}{p_{\rm i}\cdot n}+\frac{U}{c}\frac{n\cdot n_{\boldsymbol{K}}}{p_{\rm i}\cdot n}}, \tag{7}$$

such that

$$\omega_{\boldsymbol{K},N}=\frac{\omega^{\rm Th}_{\boldsymbol{K},N}}{1+\frac{\omega^{\rm Th}_{\boldsymbol{K},N}}{\omega_{\rm cut}}}. \tag{8}$$

Note that, for a given geometry of the process and for a given initial electron momentum, the Thomson frequencies are equally separated from each other. The same is not true for the Compton frequencies. This scaling law, which relates the quantum Compton frequency $\omega_{\boldsymbol{K},N}$ to its classical analog, the Thomson frequency $\omega^{\rm Th}_{\boldsymbol{K},N}$, has been discussed recently for

*Katarzyna.Krajewska@fuw.edu.pl

long laser pulses [15–17]. Its extension to short laser pulses, together with the investigation of polarization and spin effects, and the synthesis of ultrashort pulses have been presented in Ref. [18].

The Klein-Nishina formula (4) can be also expressed in the form

$$N = \frac{\omega_{\boldsymbol{K},N}\omega_{\rm cut}}{\omega(\omega_{\rm cut}-\omega_{\boldsymbol{K},N})}\left(\frac{p_{\rm i}\cdot n_{\boldsymbol{K}}}{p_{\rm i}\cdot n}+\frac{U}{c}\frac{n\cdot n_{\boldsymbol{K}}}{p_{\rm i}\cdot n}\right), \tag{9}$$

which, for the given geometry of the scattering process and for the given frequency of the emitted Compton photon, allows us to determine the nonlinearity of the process, N. Note that the quantum nature of this formula is hidden in $\omega_{\rm cut}$. Therefore, we recover the classical result in the limit when $\omega_{\boldsymbol{K},N} \ll \omega_{\rm cut}$. Similar formulas can be derived for multichromatic plane-wave-fronted fields with commensurate frequencies.

B. Spectrally resolved Compton peaks induced by short laser pulses

If the Compton process occurs in a short and intense laser pulse, the situation is different. It follows from the time-frequency uncertainty principle that, if the driving pulse lasts for time $T_{\rm p}$, the frequency scale over which the system undergoes a significant change cannot be smaller than roughly $2\pi/T_{\rm p}$. For this reason, the individual peaks in the Compton frequency spectrum are hardly visible if the process occurs in few-cycle pulses (see, e.g., Refs. [15,16,19–21]). Now, the question arises: Is it possible to design a short laser pulse such that the individual peaks in the laser-induced Compton spectrum are clearly distinguished from each other, with unambiguously prescribed to them integer orders N? Although the answer to this question is in general negative, for suitably designed pulses, one can achieve the limit imposed by the aforementioned uncertainty relation. The idea of how to avoid the spectral broadening follows from the Fraunhoffer diffraction theory as applied to the diffraction gratings, or from the frequency comb generation, and is based on the application of modulated laser pulses [22,23]. We demonstrate in this paper that, by using this technique, it is possible to achieve the clear spectral resolution of individual peaks in the Compton spectrum, even if driven by few-cycle laser pulses.

The Compton scattering by short laser pulses is very sensitive to the precise form of the driving pulse. It was pointed out in Ref. [6] that this sensitivity can be used to characterize the driving laser field. In Ref. [6], the angular distributions of Compton radiation were traced back to the carrier-envelope phase of the driving pulse. As we point out, the spectrally resolved peaks in the Compton distribution allow for determining properties of the driving modulated pulse. This is done by mapping the positions of the Compton peaks to the GKN formula that we derive in this paper. It is important to stress that the modulated pulse is shaped such that it appears as a finite train of identical subpulses. Hence, the GKN formula is applicable to an arbitrary, finite train of identical pulses.

The paper is organized as follows. In the next section, the theory of Compton scattering in finite plane-wave-fronted pulses is presented, which is then followed by the discussion of the diffraction formula (Sec. III). In Sec. IV, we present the GKN formula. It describes the major peaks in the Compton spectrum of radiation induced by a finite train of pulses. Since the formula depends on properties of the individual pulse from the train, one may exploit the properties of the Compton spectra in the diagnostics of relativistically intense, short laser pulses. This is illustrated in Sec. V for one- and three-cycle pulses. Section VI contains concluding remarks.

In analytic formulas we keep $\hbar = 1$ and, hence, the fine-structure constant becomes $\alpha = e^2/(4\pi\varepsilon_0 c)$. Unless stated otherwise, in numerical analysis we use relativistic units (rel. units) such that $\hbar = m_{\rm e} = c = 1$, where $m_{\rm e}$ is the electron mass.

II. COMPTON SCATTERING

The probability amplitude for the Compton process, $e^-_{\boldsymbol{p}_{\rm i}\lambda_{\rm i}} \to e^-_{\boldsymbol{p}_{\rm f}\lambda_{\rm f}} + \gamma_{\boldsymbol{K}\sigma}$, with the initial and final electron momenta and spin polarizations $\boldsymbol{p}_{\rm i}\lambda_{\rm i}$ and $\boldsymbol{p}_{\rm f}\lambda_{\rm f}$, respectively, equals [21]

$$\mathcal{A}(e^-_{\boldsymbol{p}_{\rm i}\lambda_{\rm i}} \to e^-_{\boldsymbol{p}_{\rm f}\lambda_{\rm f}} + \gamma_{\boldsymbol{K}\sigma}) = -ie\int d^4x\, j^{(++)}_{\boldsymbol{p}_{\rm f}\lambda_{\rm f},\boldsymbol{p}_{\rm i}\lambda_{\rm i}}(x)\cdot A^{(-)}_{\boldsymbol{K}\sigma}(x). \tag{10}$$

Here, $\boldsymbol{K}\sigma$ denotes the Compton photon momentum and polarization, and

$$A^{(-)}_{\boldsymbol{K}\sigma}(x) = \sqrt{\frac{1}{2\varepsilon_0\omega_{\boldsymbol{K}}V}}\,\varepsilon^*_{\boldsymbol{K}\sigma}e^{iK\cdot x}, \tag{11}$$

where V is the quantization volume, $\omega_{\boldsymbol{K}} = cK^0 = c|\boldsymbol{K}|$ ($K\cdot K=0$), and $\varepsilon_{\boldsymbol{K}\sigma} = (0,\boldsymbol{\varepsilon}_{\boldsymbol{K}\sigma})$ are the polarization four-vectors satisfying the conditions $K\cdot\varepsilon_{\boldsymbol{K}\sigma}=0$ and $\varepsilon^*_{\boldsymbol{K}\sigma}\cdot\varepsilon_{\boldsymbol{K}\sigma'} = -\delta_{\sigma\sigma'}$, for $\sigma,\sigma' = 1,2$. Moreover, $j^{(++)}_{\boldsymbol{p}_{\rm f}\lambda_{\rm f},\boldsymbol{p}_{\rm i}\lambda_{\rm i}}(x)$ is the matrix element of the electron current operator with its ν component equal to

$$[j^{(++)}_{\boldsymbol{p}_{\rm f}\lambda_{\rm f},\boldsymbol{p}_{\rm i}\lambda_{\rm i}}(x)]^\nu = \bar{\psi}^{(+)}_{\boldsymbol{p}_{\rm f}\lambda_{\rm f}}(x)\gamma^\nu\psi^{(+)}_{\boldsymbol{p}_{\rm i}\lambda_{\rm i}}(x). \tag{12}$$

Here, $\psi^{(+)}_{\boldsymbol{p}\lambda}(x)$ is the Volkov solution of the Dirac equation coupled to the electromagnetic field [24].

The Volkov solution of the Dirac equation for electrons of the four-momentum $p=(p^0,\boldsymbol{p})$, $p\cdot p = m_{\rm e}^2c^2$, is of the from

$$\psi^{(+)}_{\boldsymbol{p}\lambda}(x) = \sqrt{\frac{m_{\rm e}c^2}{VE_{\boldsymbol{p}}}}\left[1-\frac{e}{2k\cdot p}\not{A}(k\cdot x)\not{k}\right]u^{(+)}_{\boldsymbol{p}\lambda}e^{-iS^{(+)}_p(x)}, \tag{13}$$

where

$$S^{(+)}_p(x) = p\cdot x + \int_0^{k\cdot x}\left[e\frac{A(\phi)\cdot p}{k\cdot p} - e^2\frac{A^2(\phi)}{2k\cdot p}\right]d\phi, \tag{14}$$

$E_{\boldsymbol{p}} = cp^0$ and $u^{(+)}_{\boldsymbol{p}\lambda}$ is the free-electron bispinor normalized such that $\bar{u}^{(+)}_{\boldsymbol{p}\lambda}u^{(+)}_{\boldsymbol{p}\lambda'} = \delta_{\lambda\lambda'}$ with $\lambda = \pm$ labeling the spin degrees of freedom. The electromagnetic vector potential $A(k\cdot x)$ is assumed to be an arbitrary function of $k\cdot x$, with $k\cdot k=0$ and $\omega = ck^0$. Let the laser pulse lasts for time $T_{\rm p}$. Therefore, by choosing $\omega = 2\pi/T_{\rm p}$ we can assume that $A(k\cdot x)$ vanishes for $k\cdot x<0$ and $k\cdot x > 2\pi$. This allows us to interpret the label $\boldsymbol{p}$ of the Volkov wave (13) as the electron momentum in the remote past or future.

In analogy to the Bloch theorem in solid-state physics, we can introduce the electron quasimomentum $\bar{p}$. It describes the electron dressing by the electromagnetic field,

$$S_p(x) = \bar{p}\cdot x + G_p(k\cdot x), \tag{15}$$

where, for the most general, elliptically polarized plane-wave-fronted pulse,

$$A(k\cdot x) = A_0[\varepsilon_1 f_1(k\cdot x) + \varepsilon_2 f_2(k\cdot x)], \tag{16}$$

the laser-dressed momentum has the form [21]

$$\bar{p} = p - \mu m_e c\left(\frac{p\cdot\varepsilon_1}{p\cdot n}\langle f_1\rangle + \frac{p\cdot\varepsilon_2}{p\cdot n}\langle f_2\rangle\right)n + \frac{1}{2}(\mu m_e c)^2\frac{\langle f_1^2\rangle + \langle f_2^2\rangle}{p\cdot n}n. \tag{17}$$

Here, the parameter μ is defined according to Eq. (6). The so-called shape functions, $f_j(k\cdot x)$, $j=1,2$, are arbitrary functions with continuous second derivatives that vanish outside the interval $(0,2\pi)$. For any of such functions $F(\phi)$, we define

$$\langle F\rangle = \frac{1}{2\pi}\int_0^{2\pi} F(\phi)d\phi. \tag{18}$$

Note that the pulses with plane wave fronts, which are considered in this paper, very well describe the interaction of laser fields with energetic electrons. This is provided that the kinetic energy of electrons is much larger than their ponderomotive energy in the laser field (see, e.g., Ref. [25]).

Our definition of the laser-dressed momentum (17) follows directly from the Volkov solution (13). For the plane wave, the polarization-dependent terms in Eq. (17) vanish, since $\langle f_j\rangle = 0$. Note that the laser-dressed momentum, as the quantity defined in the laser field, cannot be a physical observable. It follows, however, from Eqs. (13) and (15) that the difference $(\bar{p}_f - \bar{p}_i)$ (up to a four-vector proportional to k) can be directly measured in an experiment, as it uniquely determines the Compton frequency $\omega_{\boldsymbol{K}}$ [see Eq. (30) below]. This means that, in principle, we can redefine the dressed momentum (17) by adding an arbitrary four-vector that is independent of p and vanishes outside the laser pulse. By further assuming that this four-vector is not space and time dependent, and that it should be determined only by the four-vectors present in the definition of the laser pulse, one can consider the following modification [26],

$$\bar{p} \to \bar{p} + g_1\varepsilon_1 + g_2\varepsilon_2 + g_0 k, \tag{19}$$

with $g_j = 0$ in the absence of the laser field. It appears that this dressed momentum is on the mass shell (i.e., $\bar{p}\cdot\bar{p}$ is independent of p) for a particular choice of g_j,

$$g_1 = \mu m_e c\langle f_1\rangle,\quad g_2 = \mu m_e c\langle f_2\rangle,\quad g_0 = 0, \tag{20}$$

for which

$$\bar{p}\cdot\bar{p} = (\bar{m}_e c)^2 = (m_e c)^2\left[1 + \frac{2U}{m_e c^2}\right], \tag{21}$$

where $\bar{m}_e$ is called the electron dressed mass, and

$$U = \tfrac{1}{2}\mu^2 m_e c^2\left[\langle f_1^2\rangle - \langle f_1\rangle^2 + \langle f_2^2\rangle - \langle f_2\rangle^2\right]. \tag{22}$$

This result has led the authors of Ref. [27] to the conclusion that the electron mass shift in a laser field could be measured by comparing the spectrum of Compton radiation induced by two different pulses, but of the same energy. However, it follows from our analysis that the electron mass shift can be well defined *only* for the particular choice of the momentum dressing [Eqs. (19) and (20)]. This can create doubts about the physical nature of this quantity.

Indeed, the quantity defined in Eq. (22) is the direct generalization of the ponderomotive energy (5) in the electron reference frame for the finite laser pulses; in the arbitrary reference frame the ponderomotive energy can be defined as the time component of the ponderomotive four-momentum u multiplied by the speed of light c, i.e., as $U = cu^0$, where (cf. Ref. [28] for the case when $\langle A\rangle = 0$),

$$u^\nu = -\frac{e^2}{2}\frac{\langle A\cdot A\rangle - \langle A\rangle\cdot\langle A\rangle}{p\cdot k}k^\nu. \tag{23}$$

This allows us to define the dressed mass in the relativistically invariant form [29],

$$\bar{m}_e^2 = \frac{1}{c^2}(p+u)^2, \tag{24}$$

which is independent of both the electron momentum p and the fundamental frequency ω, as well as of the laser pulse polarization vectors ε_j. Equation (24), among others, has lead Reiss [29] to the critique of the concept of the electron mass shift in a laser field. Note that such a dressing does not follow from the prescription (19) if the parameters g_j are p independent and, in general, cannot be related to the "quasimomentum" for the Volkov solution.

It is not the purpose of this paper to take part in the discussion concerning the mass shift. However, independent of the physical interpretation, both the mass shift and the ponderomotive momentum are uniquely defined by particular laser pulse characteristics, namely, by $\mu^2(\langle f_1^2\rangle + \langle f_2^2\rangle)$ and $\mu\langle f_j\rangle$ for $j=1,2$. It appears that also the Compton photon frequency depends on them (see, e.g., Eqs. (29) and (30) in Ref. [18]). This indicates that there should exist an experimental method which allows us to determine these parameters from direct measurements of the frequency spectrum of Compton photons. This would allow us to determine either mass shift or the ponderomotive momentum of the electron in the laser field. It could be also used for the analysis of the peak intensity, the carrier-envelope phase, or polarization properties of very intense, short laser pulses.

In this context, we further analyze the probability amplitude for the Compton process (10) and rewrite it as

$$\mathcal{A}(e^-_{\boldsymbol{p}_i\lambda_i} \longrightarrow e^-_{\boldsymbol{p}_f\lambda_f} + \gamma_{\boldsymbol{K}\sigma}) = i\sqrt{\frac{2\pi\alpha c(m_e c^2)^2}{E_{\boldsymbol{p}_f}E_{\boldsymbol{p}_i}\omega_{\boldsymbol{K}}V^3}}\,\mathcal{A}, \tag{25}$$

where

$$\mathcal{A} = \int d^4x\,\bar{u}^{(+)}_{\boldsymbol{p}_f\lambda_f}\left(1 - \mu\frac{m_e c}{2p_f\cdot k}f_1(k\cdot x)\not{\varepsilon}_1\not{k} - \mu\frac{m_e c}{2p_f\cdot k}f_2(k\cdot x)\not{\varepsilon}_2\not{k}\right)\not{\varepsilon}^*_{\boldsymbol{K}\sigma} \times\left(1 + \mu\frac{m_e c}{2p_i\cdot k}f_1(k\cdot x)\not{\varepsilon}_1\not{k} + \mu\frac{m_e c}{2p_i\cdot k}f_2(k\cdot x)\not{\varepsilon}_2\not{k}\right)u^{(+)}_{\boldsymbol{p}_i\lambda_i}e^{-iS(x)}, \tag{26}$$

with $S(x) = S^{(+)}_{p_i}(x) - S^{(+)}_{p_f}(x) - K\cdot x$. This phase can be represented as $S(x) = (\bar{p}_i - \bar{p}_f - K)\cdot x + G(k\cdot x)$, with the laser-dressed momenta of the initial and final electrons defined according to Eq. (17). The remaining portion of the phase, $G(k\cdot x)$, is a periodic function of its argument and is given by Eq. (43) of Ref. [21]. Next, we introduce a Fourier series expansion as specified by Eq. (21) in Ref. [21]. In doing so, we use the Boca-Florescu transformation [19] which allows us to regularize the integral $\int d^4x\, e^{-iS(x)}$, that is multiplied in Eq. (26) by $\bar{u}^{(+)}_{\boldsymbol{p}_f\lambda_f}\not{\varepsilon}^*_{\boldsymbol{K}\sigma}u^{(+)}_{\boldsymbol{p}_i\lambda_i}$. The Fourier decomposition makes it possible to represent $\mathcal{A}$ in the form given by Eq. (22) of Ref. [21]. This leads to

$$\mathcal{A} = \sum_N (2\pi)^3\delta^{(1)}(P_N^-)\delta^{(2)}(\boldsymbol{P}_N^\perp)D_N\frac{1-e^{-2\pi i P_N^+/k^0}}{iP_N^+}, \tag{27}$$

where

$$P_N = \bar{p}_i + Nk - \bar{p}_f - K \tag{28}$$

and the coefficients D_N are defined in Ref. [21] by Eqs. (23) and (44). Note that the δ functions in Eq. (27) determine the respective conservation conditions. They can be rewritten in the form

$$(\bar{p}_i - \bar{p}_f - K)\cdot n = 0, \quad \bar{\boldsymbol{p}}_i^\perp - \bar{\boldsymbol{p}}_f^\perp - \boldsymbol{K}^\perp = \boldsymbol{0}, \tag{29}$$

where, for an arbitrary four-vector a, we define $\boldsymbol{a}^\perp = \boldsymbol{a} - (\boldsymbol{a}\cdot\boldsymbol{n})\boldsymbol{n}$. As a consequence, the Compton frequency,

$$\omega_{\boldsymbol{K}} = c\frac{(K\cdot n)^2 + (\boldsymbol{K}^\perp)^2}{2K\cdot n} = c\frac{[(\bar{p}_i - \bar{p}_f)\cdot n]^2 + (\bar{\boldsymbol{p}}_i^\perp - \bar{\boldsymbol{p}}_f^\perp)^2}{2(\bar{p}_i - \bar{p}_f)\cdot n}, \tag{30}$$

is uniquely defined by the difference of dressed momenta, $(\bar{p}_f - \bar{p}_i)$. For this reason one can select any form of the electron momentum dressing. Below, we adopt our definition, Eq. (17), as for such a choice the following equations hold: $\bar{p}\cdot n = p\cdot n$, $\bar{p}\cdot\varepsilon_j = p\cdot\varepsilon_j$, and $\bar{\boldsymbol{p}}^\perp = \boldsymbol{p}^\perp$, that significantly simplify analytical calculations. Based on Eqs. (25) and (27), we derive that the frequency-angular distribution of energy of the emitted photons for an unpolarized and monoenergetic electron beam is given by

$$\frac{d^3E_C}{d\omega_{\boldsymbol{K}}d^2\Omega_{\boldsymbol{K}}} = \frac{1}{2}\sum_{\sigma=1,2}\sum_{\lambda_i=\pm}\sum_{\lambda_f=\pm}\frac{d^3E_{C,\sigma}(\lambda_i,\lambda_f)}{d\omega_{\boldsymbol{K}}d^2\Omega_{\boldsymbol{K}}}. \tag{31}$$

Here,

$$\frac{d^3E_{C,\sigma}(\lambda_i,\lambda_f)}{d\omega_{\boldsymbol{K}}d^2\Omega_{\boldsymbol{K}}} = \alpha|\mathcal{A}_{C,\sigma}(\omega_{\boldsymbol{K}},\lambda_i,\lambda_f)|^2, \tag{32}$$

where the scattering amplitude equals

$$\mathcal{A}_{C,\sigma}(\omega_{\boldsymbol{K}},\lambda_i,\lambda_f) = \frac{m_e c K^0}{2\pi\sqrt{p_i^0 k^0 (k\cdot p_f)}} \times \sum_N D_N \frac{1-e^{-2\pi i(N-N_{\rm eff})}}{i(N-N_{\rm eff})}, \tag{33}$$

with $N_{\rm eff} = (K^0 + \bar{p}_f^0 - \bar{p}_i^0)/k^0$. These formulas have been derived by integrating $|\mathcal{A}(e^-_{\boldsymbol{p}_i\lambda_i} \longrightarrow e^-_{\boldsymbol{p}_f\lambda_f} + \gamma_{\boldsymbol{K}\sigma})|^2$ over the final electron states. Therefore, even though we write explicitly p_f in these formulas, one has to understand that p_f is determined by the conservation conditions (29).

In the following, we consider the linearly polarized laser pulse such that, for $0 \le \phi = k\cdot x \le 2\pi$, the vector potential has a general form $A(\phi) = A_0\varepsilon f(\phi)$ [i.e., we put $\varepsilon = \varepsilon_1$, $f(\phi) = f_1(\phi)$, and $f_2(\phi) = 0$] and the electric field vector equals $\boldsymbol{\mathcal{E}}(\phi) = -\omega A_0\boldsymbol{\varepsilon}f'(\phi)$. The shape function $f(\phi)$ is defined via its derivative,

$$f'(\phi) = \begin{cases} 0, & \phi < 0, \\ N'_f \sin^2\left(N_{\rm rep}\frac{\phi}{2}\right)\sin(N_{\rm rep}N_{\rm osc}\phi), & 0 \le \phi \le 2\pi, \\ 0, & \phi > 2\pi, \end{cases} \tag{34}$$

where we assume that $f(0) = 0$. Note that this pulse consists of $N_{\rm rep}$ identical subpulses, with $N_{\rm osc}$ cycles each. Regardless of its interpretation as a finite train of pulses, it is justified to apply the theory derived in Ref. [21] for the process driven by a single pulse, which was recapitulated in the previous paragraph. Since the modulated pulse (34) lasts for time T_p, we can define its fundamental, $\omega = 2\pi/T_p$, and its central frequency, $\omega_L = N_{\rm rep}N_{\rm osc}\omega$. The latter is supposed to be fixed and equal to $\omega_L = 1.55$ eV $\approx 3\times 10^{-6}\, m_e c^2$ in all calculations performed below. In the following, we assume that $N'_f = N_{\rm rep}N_{\rm osc}$. This guarantees that the time-averaged intensity carried out by the laser field is independent of $N_{\rm rep}$ and $N_{\rm osc}$, as for this particular choice of N'_f the amplitude of the electric field scales as $\omega_L\mu$. Note that, for the rectangular pulse, the $\sin^2$ envelope is not present in Eq. (34). Therefore, in this case the laser pulse depends only on the product $N_{\rm rep}N_{\rm osc}$.

In analogy to the original Klein-Nishina formula [Eqs. (4) and (9)], we present the frequency spectrum as a function of $\mathcal{N}$,

$$\mathcal{N} = \frac{\omega_{\boldsymbol{K}}\omega_{\rm cut}}{\omega_L(\omega_{\rm cut} - \omega_{\boldsymbol{K}})}\left(\frac{p_i\cdot n_{\boldsymbol{K}}}{p_i\cdot n} + \frac{U}{c}\frac{n\cdot n_{\boldsymbol{K}}}{p_i\cdot n}\right). \tag{35}$$

In this case, we expect that in the limit of a very long pulse the peaks in the spectrum will appear for $\mathcal{N}$'s very close to integers, as it indeed takes place for a monochromatic plane wave.

In Fig. 1, we present the angular-resolved distributions of Compton radiation [Eq. (31)] generated by a single pulse, with $N_{\rm osc} = 30$ field oscillations. This distribution is presented as the function of $\mathcal{N}$. One could expect that, for such a long driving pulse, the Klein-Nishina formula could be successfully used and that the dominant peaks would correspond to integer values of $\mathcal{N}$. Clearly, we do not observe such a behavior as the peaks are red-shifted, independently of the Compton photon polarization. As we show in the next section, the situation is changed when a train of incident pulses is considered.

III. DIFFRACTION FORMULA

It was shown in Ref. [23] that, for a finite train of pulses, the Compton probability amplitude has the diffraction-type form,

$$\mathcal{A}_{C,\sigma}(\omega_{\boldsymbol{K}},\lambda_i,\lambda_f) = \exp[i\Phi_{C,\sigma}(\omega_{\boldsymbol{K}},\lambda_i,\lambda_f)] \times \frac{\sin(\pi\bar{Q}^+/k^0)}{\sin(\pi\bar{Q}^+/k^0N_{\rm rep})}\left|\mathcal{A}^{(1)}_{C,\sigma}(\omega_{\boldsymbol{K}},\lambda_i,\lambda_f)\right|, \tag{36}$$

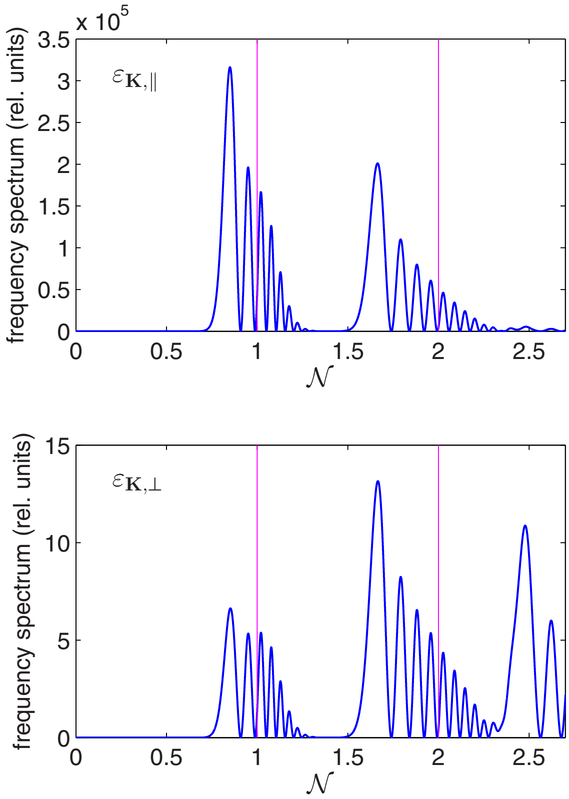

FIG. 1. (Color online) Shows the spectra of Compton radiation [Eq. (31)] resulting from the head-on collision of the linearly polarized laser pulse and an electron of momentum $\boldsymbol{p}_{\rm i} = -10^3 m_{\rm e}c\boldsymbol{e}_z$. The laser pulse ($\mu = 1$ and $\omega_{\rm L} = 1.55$ eV) propagates along the z direction and is polarized along the x direction. These two axes determine the scattering plane. The pulse has a $\sin^2$ envelope [Eq. (34)] with $N_{\rm osc} = 30$ and $N_{\rm rep} = 1$. The Compton photon is emitted in the direction of $\theta_{\boldsymbol{K}} = 0.9999\pi$ and $\varphi_{\boldsymbol{K}} = \pi$, with the polarization vector either parallel (upper panel) or perpendicular to the scattering plane (lower panel). The energy spectra are presented as functions of $\mathcal{N}$, where the vertical lines mark the integer values of this argument. For this particular kinematics of the scattering process, the frequency of emitted photons $\omega_{\boldsymbol{K}}$ almost linearly depends on $\mathcal{N}$, namely, $\omega_{\boldsymbol{K}} \approx 9.33\mathcal{N} m_{\rm e}c^2$.

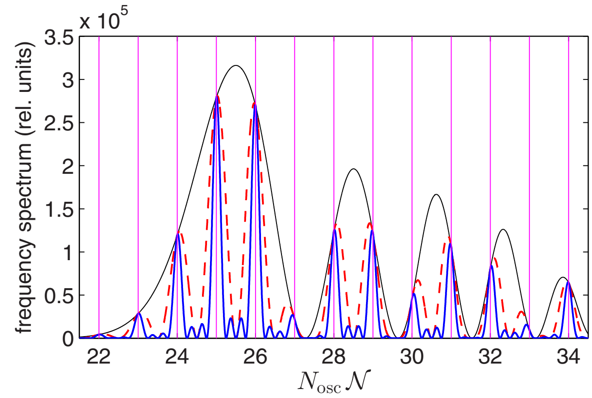

FIG. 2. (Color online) The same as in Fig. 1 but only for the Compton photon polarized in the scattering plane. We show the spectra for $N_{\rm rep} = 1$ (black envelope), $N_{\rm rep} = 2$ (dashed red [gray] line), and $N_{\rm rep} = 4$ (solid blue [gray] line). The vertical lines mark the integer values of $N_{\rm osc}\mathcal{N}$, for which we observe the approximate positions of peaks for $N_{\rm rep} > 1$.

where $\mathcal{A}^{(1)}_{{\rm C},\sigma}$ is the Compton amplitude for a single pulse and $\Phi_{{\rm C},\sigma}(\omega_{\boldsymbol{K}},\lambda_{\rm i},\lambda_{\rm f})$ is the Compton global phase. In the above equation $\bar{Q}^+ = \bar{p}_{\rm i}^+ - \bar{p}_{\rm f}^+ - K^+$ where, for an arbitrary four-vector a, we define $a^+ = a^0 - (a\cdot n)/2 = (a^0 + \boldsymbol{a}\cdot\boldsymbol{n})/2$. For particular frequencies of emitted photons ($\omega_{\boldsymbol{K},N}$ with integer N), that satisfy the condition

$$\pi\bar{Q}^+ = -\pi N N_{\rm rep} k^0, \tag{37}$$

we observe the coherent enhancement of the Compton amplitude. This, in turn, leads to the quadratic, $N_{\rm rep}^2$, enhancement of the respective probability distribution. In contrast to the classical Thomson process, these frequencies are not *exactly* equally spaced in the allowed frequency region, $0 < \omega_{\boldsymbol{K}} < \omega_{\rm cut}$. When $\omega_{\boldsymbol{K}}$ approaches the cutoff value $\omega_{\rm cut}$ [Eq. (2)], i.e., when the quantum recoil of the scattered electron cannot be neglected, the spectrum of $\omega_{\boldsymbol{K},N}$ becomes increasingly denser. This means that one can generate the Compton-based frequency combs with equidistant peak frequencies only within limited frequency intervals.

The Compton global phase equals

$$\Phi_{{\rm C},\sigma}(\omega_{\boldsymbol{K}},\lambda_{\rm i},\lambda_{\rm f}) = -\pi\frac{\bar{Q}^+}{k^0} + \Phi^{\rm dyn}_{{\rm C},\sigma}(\omega_{\boldsymbol{K}},\lambda_{\rm i},\lambda_{\rm f}), \tag{38}$$

where $\Phi^{\rm dyn}_{{\rm C},\sigma}$ is the so-called dynamic phase [23]. For arbitrary laser pulses and polarizations of emitted photons, the dynamic phase can only be calculated numerically. It happens that, for pulses considered in this paper, the dynamic phase is independent of $\omega_{\boldsymbol{K}}$. This means that, for frequencies $\omega_{\boldsymbol{K},N}$ satisfying the condition (37), the global phase is equal to

$$\Phi_{{\rm C},\sigma}(\omega_{\boldsymbol{K},N},\lambda_{\rm i},\lambda_{\rm f}) = \pi N N_{\rm rep} + \Phi^{\rm dyn}_{{\rm C},\sigma}(\omega_{\boldsymbol{K},N},\lambda_{\rm i},\lambda_{\rm f}), \tag{39}$$

and, hence, it takes on the same values modulo π. The selection of these particular phases for the peak frequencies leads not only to the enhancement of the frequency spectrum but also to the synthesis of ultrashort pulses of radiation generated during the Compton scattering [30].

As an illustration, we consider the same laser pulse as in Fig. 1 but repeated $N_{\rm rep}$ times. In Fig. 2, we show the Compton spectra for $N_{\rm rep} = 1$, 2, and 4, when divided by $N_{\rm rep}^2$. The results are presented as the functions of $N_{\rm osc}\mathcal{N}$. The clearly visible peaks occur for $N_{\rm rep} > 1$. Their positions are almost independent of $N_{\rm rep}$ and they correspond to the integer values of $N_{\rm osc}\mathcal{N}$. Note that $\omega = \omega_{\rm L}/N_{\rm osc}$ is the fundamental frequency of the individual laser pulse from the train. Such a pulse can be approximately interpreted as a coherent superposition of at most $N_{\rm osc}$ photon states of frequencies $K\omega$, $K = 1,\ldots,N_{\rm osc}$ (of course, photons with other frequencies are also present, but with smaller amplitudes). Therefore, in the course of the Compton scattering, the electron can absorb these photons with the total energy $N\omega$ and emit a single photon of frequency $\omega_{\boldsymbol{K},N}$. However, due to the time-frequency uncertainty relation and an incoherent interference of probability amplitudes, the spectrum is smeared out such that it is not possible to clearly prescribe peaks to integer orders N. This is clearly seen in Figs. 1 and 2. The situation changes if we consider the sequence of at least two such pulses. Now, due to the constructive interference, the processes with integer $N_{\rm osc}\mathcal{N}$ are coherently enhanced. As a result, we observe in the spectrum the clearly resolved peaks already for $N_{\rm rep}=2$.

The coherent enhancement of the Compton frequency spectra does not take place for a single pulse with the time-varying envelope. It appears, however, that important features of a single pulse can be precisely determined from positions of the main diffraction peaks in the Compton spectrum, when generated by a train of such pulses.

IV. GENERALIZED KLEIN-NISHINA FORMULA

As we have demonstrated above, the application of the pulse train with two subpulses already allows us to increase the resolution of the frequency spectrum of Compton radiation such that one can unambiguously prescribe an integer number to the individual peak. We have shown this for a long pulse ($N_{\rm osc}=30$), for which $\langle f\rangle$ is negligibly small, so that the original Klein-Nishina formula may be applied. For shorter pulses, $\langle f\rangle$ starts to be significantly different than zero and the generalization of the Klein-Nishina formula, that accounts for this fact, is necessary. We apply the diffraction formula and determine the Compton photon frequency by solving the system of Eqs. (29) and (37). After some algebra, we arrive at the following GKN formula valid for a pulse train of an arbitrary polarization:

$$\omega_{\boldsymbol{K},N}^{(\rm GKN)}=\frac{(N/N_{\rm osc})\omega_{\rm L}}{\frac{p_{\rm i}\cdot n_{\boldsymbol{K}}}{p_{\rm i}\cdot n}+\frac{\nu n\cdot n_{\boldsymbol{K}}+g_1 p_{\rm i,1}+g_2 p_{\rm i,2}}{(p_{\rm i}\cdot n)^2}+\frac{(N/N_{\rm osc})\omega_{\rm L}}{\omega_{\rm cut}}}. \tag{40}$$

Here, g_1 and g_2 are defined in Eq. (20),

$$\nu=\tfrac{1}{2}(\mu m_{\rm e}c)^2\big(\langle f_1^2\rangle+\langle f_2^2\rangle\big), \tag{41}$$

and (for $j=1,2$)

$$p_{{\rm i},j}=(p_{\rm i}\cdot n)(n_{\boldsymbol{K}}\cdot\varepsilon_j)-(p_{\rm i}\cdot\varepsilon_j)(n\cdot n_{\boldsymbol{K}}). \tag{42}$$

As for the original Klein-Nishina formula, the quantum signature is hidden in the definition of $\omega_{\rm cut}$ [Eq. (2)]. The frequencies determined by Eq. (40) mark the positions of main peaks in the Compton spectrum. Similarly, one can find frequencies of the secondary peaks (if $N_{\rm rep}>2$) and zeros (if $N_{\rm rep}>1$) in the angular-resolved frequency distributions. It is worth noting that now the polarization-dependent terms appear not in the unphysical dressing of the electron initial and final momenta but in the definition of the directly measurable quantity; in other words, they affect the peak frequencies of the Compton spectrum. Similarly to the original Klein-Nishina formula we define the quantity

$$\mathcal{N}_{\rm GKN}=\frac{N_{\rm osc}\omega_{\boldsymbol{K}}\omega_{\rm cut}}{\omega_{\rm L}(\omega_{\rm cut}-\omega_{\boldsymbol{K}})}\bigg(\frac{p_{\rm i}\cdot n_{\boldsymbol{K}}}{p_{\rm i}\cdot n}+\frac{\nu n\cdot n_{\boldsymbol{K}}+g_1 p_{\rm i,1}+g_2 p_{\rm i,2}}{(p_{\rm i}\cdot n)^2}\bigg), \tag{43}$$

which acquires integer values for peak frequencies $\omega_{\boldsymbol{K},N}^{(\rm GKN)}$. For $\langle f_j\rangle=0$ and $N_{\rm osc}=1$, this formula reduces to the original one, given by Eq. (35).

The derivation of the formula (36) shows that, in order to observe a coherent enhancement of the Compton spectra, the modulations of the driving pulse cannot be arbitrary [23].

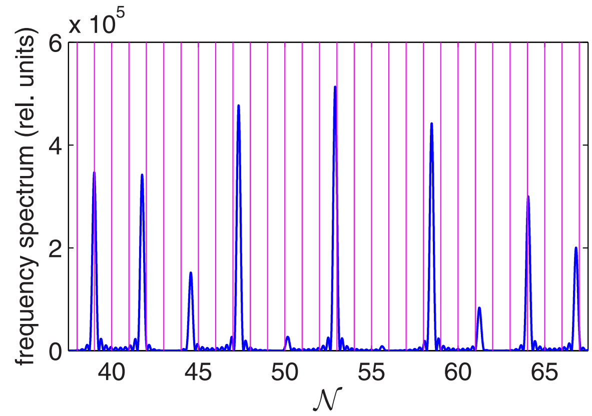

FIG. 3. (Color online) The same as in Fig. 1 but for the rectangular pulse with $N_{\rm osc}=1$ and $N_{\rm rep}=10$. The laser field intensity is characterized by the parameter $\mu=3$. The Compton photon is emitted in the direction specified by $\theta_{\boldsymbol{K}}=0.999\pi$ and $\varphi_{\boldsymbol{K}}=\pi$. The energy spectrum is presented as the function of $\mathcal{N}$ [Eq. (35)].

Both the integral of the electric field over the time duration of a single modulation and the vector potential in the beginning and at the end of it have to vanish. In other words, we have to deal with a train of pulses. This precludes the application of the diffraction formula not only to single pulses with envelopes varying in time, but also to the rectangular pulses of an arbitrary polarization. The exception is the linearly polarized rectangular pulse, but even in this case one has to redefine the vector potential such that $\langle f\rangle\neq 0$. This means that, irrespective of the duration of such a rectangular pulse, the original Klein-Nishina formula (4) is not applicable, unless the particular geometry is selected such that $p_{{\rm i},j}=0$ for $g_j\neq 0$. For instance, in the electron reference frame this happens if $\boldsymbol{n}_{\boldsymbol{K}}\cdot\boldsymbol{\varepsilon}_j=0$, as $p_{\rm i}\cdot\varepsilon_j=0$. This corresponds to the case when the Compton photon is ejected perpendicular to the laser field polarization vector.

In Figs. 3 and 4, we consider a generic case when $p_{{\rm i},j}\neq 0$ for the linearly polarized laser field. In these figures we compare the same spectrum of emitted radiation, but we present it as the function of either $\mathcal{N}$ or $\mathcal{N}_{\rm GKN}$. We see that

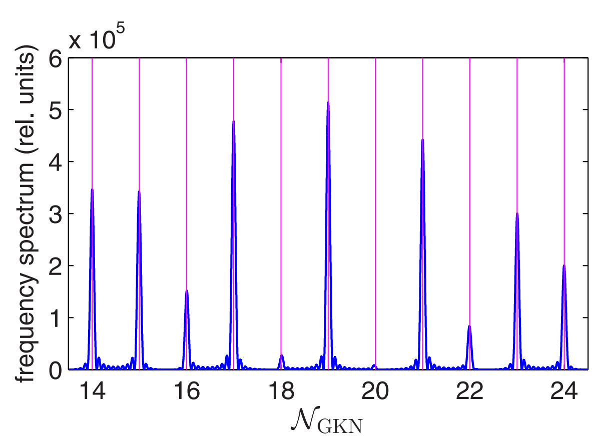

FIG. 4. (Color online) The same as in Fig. 3, but the spectrum is plotted as a function of $\mathcal{N}_{\rm GKN}$ [Eq. (43)].

the main peaks of this spectrum correspond exactly to the integer values of $\mathcal{N}_{\rm GKN}$. We also observe a dramatic difference in numerical values for $\mathcal{N}$ and $\mathcal{N}_{\rm GKN}$. For instance, the first peak corresponds to $\mathcal{N}=39$ or $\mathcal{N}_{\rm GKN}=14$. If the original Klein-Nishina formula had been used for interpreting this peak one would ascribe it to the process with absorption of 39 laser photons (not accounting for the fact that the majority of the peaks could not be interpreted this way, since they do not match the integer values of $\mathcal{N}$). In contrast, for the GKN formula, all the main peaks can be interpreted as the result of absorption of an integer number of laser photons. Note that the positions of these peaks are the same with the increasing $N_{\rm rep}$, whereas their widths become increasingly narrower.

The positions of the interference peaks, as represented in Fig. 4, allow to determine parameters of the driving laser field. In order to demonstrate this, we define the quantities

$$\eta = \nu n\cdot n_{\boldsymbol K} + g_1 p_{{\rm i},1} + g_2 p_{{\rm i},2}, \tag{44}$$

$$A(\omega_{\boldsymbol K}) = \frac{N_{\rm osc}\omega_{\boldsymbol K}\omega_{\rm cut}}{\omega_{\rm L}(\omega_{\rm cut}-\omega_{\boldsymbol K})(p_{\rm i}\cdot n)^2}, \tag{45}$$

$$B(\omega_{\boldsymbol K}) = \frac{N_{\rm osc}\omega_{\boldsymbol K}\omega_{\rm cut}}{\omega_{\rm L}(\omega_{\rm cut}-\omega_{\boldsymbol K})}\,\frac{p_{\rm i}\cdot n_{\boldsymbol K}}{p_{\rm i}\cdot n}. \tag{46}$$

These quantities depend on the initial electron energy and the geometry of the scattering process. Except for η, they also depend on the frequency of emitted photons. The latter means that, for a given frequency distribution, η remains constant. Moreover, only η depends on the laser pulse parameters such as $\mu^2(\langle f_1^2\rangle + \langle f_2^2\rangle)$ and $\mu\langle f_j\rangle$ for both linear polarizations (note that only these parameters are necessary for the determination of the electron effective mass or the ponderomotive four-momentum, as discussed in Sec. II). Using the above definitions, Eq. (43) can be rewritten as

$$A(\omega_{\boldsymbol K})\eta = \mathcal{N}_{\rm GKN} - B(\omega_{\boldsymbol K}). \tag{47}$$

This equation determines η provided that we can unambiguously prescribe an integer number to an arbitrarily chosen peak frequency. Let us choose two consecutive peaks from the spectrum, i.e., $\omega^{\rm (GKN)}_{{\boldsymbol K},N}$ and $\omega^{\rm (GKN)}_{{\boldsymbol K},N+1}$. By solving the system of two equations, each having the form (47) for the given peak frequency, we obtain that

$$\eta = \frac{1 - B\big(\omega^{\rm (GKN)}_{{\boldsymbol K},N+1}\big) + B\big(\omega^{\rm (GKN)}_{{\boldsymbol K},N}\big)}{A\big(\omega^{\rm (GKN)}_{{\boldsymbol K},N+1}\big) - A\big(\omega^{\rm (GKN)}_{{\boldsymbol K},N}\big)}. \tag{48}$$

This quantity should be independent of N. For instance, the frequencies of the first two peaks in Fig. 4, which have been estimated from the graph, are $\omega^{\rm (GKN)}_{{\boldsymbol K},14}\approx 29.817 m_{\rm e}c^2$ and $\omega^{\rm (GKN)}_{{\boldsymbol K},15}\approx 31.878 m_{\rm e}c^2$. They result in $\eta\approx -5.3497(m_{\rm e}c)^2$, which is very close to the exact value $\eta\approx -5.3496(m_{\rm e}c)^2$. Note that the result for η is the same for an arbitrary pair of such peak intensities. This means that in order to determine three independent parameters ν, g_1, and g_2, which appear in the definition of η [Eq. (44)], we should repeat this procedure for different geometries. For the linearly polarized laser field considered in this paper, we can determine η exactly in the same way for different angles of emission. For instance, by choosing $\theta_{\boldsymbol K}=0.9999\pi$ with all other parameters unchanged, we obtain $\eta\approx 11.615(m_{\rm e}c)^2$. These two values for η lead to the results very close to the exact values $\langle f_1^2\rangle = 1.5$ and $\langle f_1\rangle = 1$.

V. FEW-CYCLE LASER PULSES

A closer look at Fig. 2 shows that, for $N_{\rm rep}>1$, some peaks in the spectrum do not scale as $N_{\rm rep}^2$. This concerns peaks located close to the frequencies for which the distribution for the single pulse vanishes. As one can see, after dividing these distributions by $N_{\rm rep}^2$, the spectrum for $N_{\rm rep}=1$ represents the envelope for the main diffraction peaks (i.e., observed for $N_{\rm rep}>1$). This means that the spectra are tangent to each other for frequencies close to the main peaks. If the Compton spectrum for a single pulse shows rapid modulations and the diffraction peak is located at the edge of a particular modulation, then the peak frequency does not correspond to the one for which the spectra are tangent. In these cases, it may happen that the application of a pulse train does not enhance, but rather suppresses, the generated radiation. This is the reason why in Fig. 4 some of the diffraction peaks are hardly visible. To avoid the suppression of emitted radiation, it is advisable to use such laser pulses, or such scattering kinematics, so that the spectrum originating from a single pulse exhibits a broad structure, the so-called supercontinuum. Note that the formation of supercontinua was discussed recently

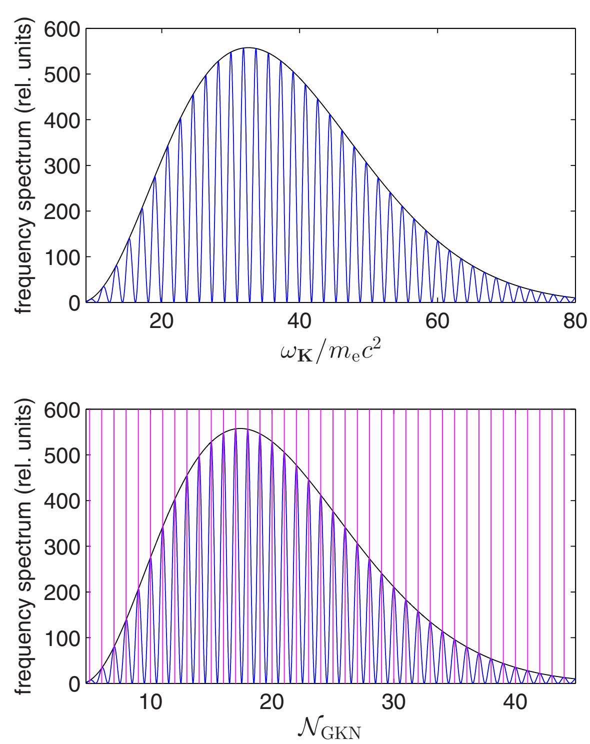

FIG. 5. (Color online) The same as in Fig. 1, but for $N_{\rm osc}=1$ and only for the Compton photon polarized in the scattering plane. The curves in each panel represent two cases: $N_{\rm rep}=1$ (smooth envelope) and $N_{\rm rep}=2$ (densely distributed peaks). In the upper panel the energy spectra are presented as functions of the Compton photon frequency $\omega_{\boldsymbol K}$, whereas in the lower frame they are presented as functions of $\mathcal{N}_{\rm GKN}$. The vertical lines in the lower panel mark the integer values of $\mathcal{N}_{\rm GKN}$, that exactly coincide with the positions of peaks. The distance between the peaks is roughly $1.79 m_{\rm e}c^2$.

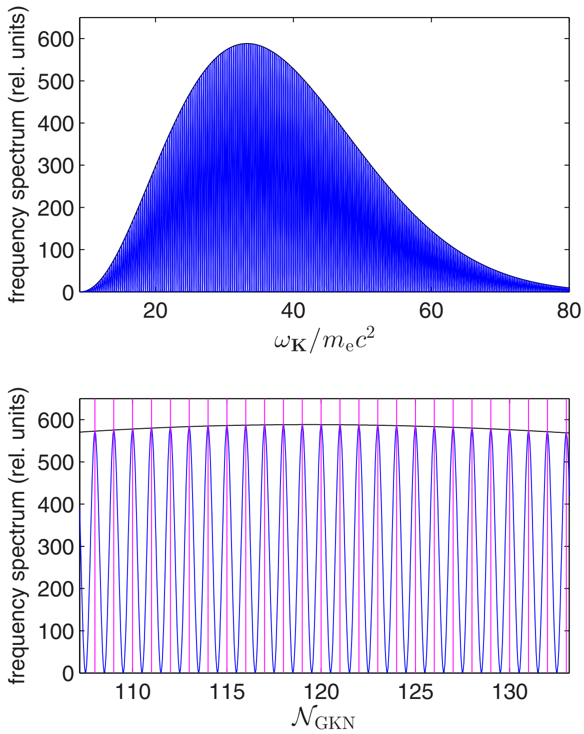

FIG. 6. (Color online) The same as in Fig. 5, but for $N_{\rm osc}=3$. Since the peaks are denser, in the lower panel only part of the spectrum is presented. The peaks are separated by roughly $0.33 m_e c^2$.

in the context of Thomson and Compton scattering, and the synthesis of zepto- and yoctosecond pulses of radiation [30]. It appears that the best choice for their generation is to use few-cycle laser pulses. We illustrate this below for $N_{\rm osc}=1$ and 3.

In Fig. 5, we present the Compton spectrum induced by a single-cycle pulse. The spectrum consists of the broad supercontinuum which extends from nearly $10 m_e c^2$ up to $80 m_e c^2$. If we repeat this pulse, $N_{\rm rep}=2$, we observe the formation of the diffraction peaks for integer values of $\mathcal{N}_{\rm GKN}$ (lower panel), which proves the validity of the GKN formula. For larger values of $N_{\rm rep}$, the positions of the main peaks stay the same but their widths become more narrow. The energy separation between the adjacent peaks is nearly the same ($\sim 1.79 m_e c^2$). Note that the pulse train under consideration is the superposition of two plane waves of frequencies $\omega_{\rm L}$ and $2\omega_{\rm L}$. Also, the peak intensity of the laser field is not very large, as it does not exceed 10^{19} W/cm^2. This suggests that our theoretical predictions could be verified experimentally, for instance, at the ELI facility [31].

For pulses with more oscillations, the situation is similar. In Fig. 6, we show this for $N_{\rm osc}=3$. The only difference is that now the distribution of the diffraction peaks is denser, with the energy separation of roughly $0.33 m_e c^2$. As above, the main peaks (for $N_{\rm rep}=2$ there are only the main diffraction peaks and the weaker secondary ones show up for $N_{\rm rep}>2$, as presented in Fig. 2) correspond to the clearly prescribed integer values of $\mathcal{N}_{\rm GKN}$. This, again, proves the validity of the GKN formula derived in this paper.

It follows from Eq. (43) that, knowing the geometry of the Compton scattering and the electron initial energy, measuring frequencies of only two consecutive peaks in the spectrum (for $N_{\rm rep}>1$) for two geometries leads to the determination of the two important parameters of linearly polarized pulses which comprise the train: $\mu^2\langle f^2\rangle$ and $\mu\langle f\rangle$ [by applying the procedure similar to that presented in Sec. IV]. If the form of the envelope is known, such measurements allow us to determine the peak intensity of incident pulses, which is characterized by the parameter μ. Another possibility is to map the positions of the Compton peaks to the carrier envelope phase, assuming that the envelope type and the peak intensity are known. Similar measurements for three different geometries can extract the values of $\mu^2(\langle f_1^2\rangle+\langle f_2^2\rangle)$ and $\mu\langle f_j\rangle$ ($j=1,2$) for elliptically polarized driving pulses and, hence, also their polarization properties.

VI. CONCLUSIONS

We have demonstrated that, by using a train consisting of a finite number of identical pulses, one can generate the Compton radiation with well-resolved peaks. In other words, we propose the mechanism to reduce the spectral broadening of the emitted radiation which typically occurs if a few-cycle pulse interacts with the electron (see, for instance, Refs. [15,16,18–21]). This is a complementary proposal to the one presented in Ref. [32–34], where a single but chirped initial pulse was used in order to compensate for the spectral broadening. Based on this result, we have derived the generalized Klein-Nishina formula.

The GKN formula (43) predicts the positions of well-resolved peaks in the Compton spectrum, when driven by a finite train of pulses. We argue that, by analyzing the positions of the peaks in the frequency domain of Compton photons, it is possible to determine laser pulse parameters, $\mu^2(\langle f_1^2\rangle+\langle f_2^2\rangle)$ and $\mu\langle f_j\rangle$ for both linear polarizations. This means that the proposed method can be applied, for instance, to determine polarization properties of such pulses and either their peak intensity or their carrier-envelope phase. Note that a similar analysis can be carried out for other fundamental processes of strong-field quantum electrodynamics, like the laser-induced Breit-Wheeler and Bethe-Heitler pair creation. These possibilities are under investigation now.

ACKNOWLEDGMENTS

This work is supported by the Polish National Science Center (NCN) under Grant No. 2012/05/B/ST2/02547. Moreover, K.K. acknowledges the support from the Kosciuszko Foundation and F.C.V. acknowledges the Foundation for Polish Science International Ph.D. Projects Programme cofinanced by the EU European Regional Development Fund.

[1] V. Yanovsky, V. Chvykov, G. Kalinchenko, P. Rousseau, T. Planchon, T. Matsuoka, A. Maksimchuk, J. Nees, G. Chieriaux, G. Mourou, and K. Krushelnick, Opt. Express **16**, 2109 (2008).

[2] A. Link, E. A. Chowdhury, J. T. Morrison, V. M. Ovchinnikov, D. Offermann, L. Van Woerkom, R. R. Freeman, J. Pasley, E. Shipton, F. Beg, P. Rambo, J. Schwarz, M. Geissel, A. Edens, and J. L. Porter, Rev. Sci. Instrum. **77**, 10E723 (2006).

[3] S.-W. Bahk, P. Rousseau, T. A. Planchon, V. Chvykov, G. Kalintchenko, A. Maksimchuk, G. A. Mourou, and V. Yanovsky, Opt. Lett. **29**, 2837 (2004).

[4] H. G. Hetzheim and C. H. Keitel, Phys. Rev. Lett. **102**, 083003 (2009).

[5] J. Gao, Appl. Phys. Lett. **88**, 091105 (2006).

[6] F. Mackenroth, A. Di Piazza, and C. H. Keitel, Phys. Rev. Lett. **105**, 063903 (2010).

[7] O. Har-Shemesh and A. Di Piazza, Opt. Lett. **37**, 1352 (2012).

[8] O. Klein and Y. Nishina, Z. Phys. **52**, 853 (1929).

[9] L. S. Brown and T. W. B. Kibble, Phys. Rev. **133**, A705 (1964).

[10] V. I. Ritus, Trudy FIAN **111**, 5 (1979).

[11] V. I. Ritus, J. Sov. Laser Res. **6**, 497 (1985).

[12] F. Ehlotzky, K. Krajewska, and J. Z. Kamiński, Rep. Prog. Phys. **72**, 046401 (2009).

[13] A. Di Piazza, C. Müller, K. Z. Hatsagortsyan, and C. H. Keitel, Rev. Mod. Phys. **84**, 1177 (2012).

[14] V. N. Nedoreshta, S. P. Roshchupkin, and A. I. Voroshilo, Laser Phys. **23**, 055301 (2013).

[15] T. Heinzl, D. Seipt, and B. Kämpfer, Phys. Rev. A **81**, 022125 (2010).

[16] D. Seipt and B. Kämpfer, Phys. Rev. A **83**, 022101 (2011).

[17] D. Seipt and B. Kämpfer, Phys. Rev. Spec. Top.—Accel. Beams **14**, 040704 (2011).

[18] K. Krajewska and J. Z. Kamiński, Phys. Rev. A **90**, 052117 (2014).

[19] M. Boca and V. Florescu, Phys. Rev. A **80**, 053403 (2009).

[20] F. Mackenroth and A. Di Piazza, Phys. Rev. A **83**, 032106 (2011).

[21] K. Krajewska and J. Z. Kamiński, Phys. Rev. A **85**, 062102 (2012).

[22] K. Krajewska and J. Z. Kamiński, Laser Phys. Lett. **11**, 035301 (2014).

[23] K. Krajewska, M. Twardy, and J. Z. Kamiński, Phys. Rev. A **89**, 052123 (2014).

[24] D. M. Volkov, Z. Phys. **94**, 250 (1935).

[25] K. Lee, S. Y. Chung, S. H. Park, Y. U. Jeong, and D. Kim, Europhys. Lett. **89**, 64006 (2010).

[26] K. Krajewska and J. Z. Kamiński, Phys. Rev. A **86**, 052104 (2012).

[27] C. Harvey, T. Heinzl, A. Ilderton, and M. Marklund, Phys. Rev. Lett. **109**, 100402 (2012).

[28] K. Krajewska and J. Z. Kamiński, Phys. Rev. A **85**, 043404 (2012).

[29] H. R. Reiss, Phys. Rev. A **89**, 022116 (2014).

[30] K. Krajewska, M. Twardy, and J. Z. Kamiński, Phys. Rev. A **89**, 032125 (2014).

[31] www.eli-laser.eu.

[32] I. Ghebregziabher, B. A. Shadwick, and D. Umstadter, Phys. Rev. Spec. Top.—Accel. Beams **16**, 030705 (2013).

[33] B. Terzić, K. Deitrick, A. S. Hofler, and G. A. Krafft, Phys. Rev. Lett. **112**, 074801 (2014).

[34] D. Seipt, S. G. Rykovanov, A. Surzhykov, and S. Fritzsche, Phys. Rev. A **91**, 033402 (2015).